forests

MDPI

Review

Advances in Global Remote Sensing Monitoring of Discolored Pine Trees Caused by Pine Wilt Disease: Platforms, Methods, and Future Directions

Hao Shi [1,2], Liping Chen [2,*], Meixiang Chen [1], Danzhu Zhang [1,2], Qiangjia Wu [1] and Ruirui Zhang [1,*]

[1] Research Center for Intelligent Equipment, Beijing Academy of Agriculture and Forestry Sciences, Beijing 100097, China; sh1053002601@163.com (H.S.); chenmx@nercita.org.cn (M.C.); zhang_danzhu@163.com (D.Z.); qiangjia@nwafu.edu.cn (Q.W.)

[2] School of Mechanical and Electrical Engineering, Gansu Agricultural University, Lanzhou 730070, China

* Correspondence: chenlp@nercita.org.cn (L.C.); zhangrr@nercita.org.cn (R.Z.)

Abstract: Pine wilt disease (PWD), caused by pine wood nematodes, is a major forest disease that poses a serious threat to global pine forest resources. Therefore, the prompt identification of PWD-discolored trees is crucial for controlling its spread. Currently, remote sensing is the primary approach for monitoring PWD. This study comprehensively reviews advances in the global remote sensing monitoring of PWD. It explores the remote sensing platforms and identification methods used in the detection of PWD-discolored trees, evaluates their precision, and provides prospects for existing problems. Three observations were made from existing studies: First, unmanned aerial vehicles (UAVs) are the dominant remote sensing platforms, and RGB data sources are the most commonly used for identifying PWD-discolored trees. Second, deep-learning methods are increasingly applied to identify PWD-discolored trees. Third, the early monitoring of PWD-discolored trees has gained increasing attention. This study reveals the problems associated with the acquisition of remote sensing images and identification algorithms. Future research directions include the fusion of multiple sensors to enhance the identification precision and early monitoring of PWD-discolored trees to obtain an optimal detection window period. This study aimed to provide technical references and scientific foundations for the comprehensive monitoring and control of PWD.

Keywords: pine wilt disease; discolored trees; identification; remote sensing; deep learning

check for updates

Citation: Shi, H.; Chen, L.; Chen, M.; Zhang, D.; Wu, Q.; Zhang, R. Advances in Global Remote Sensing Monitoring of Discolored Pine Trees Caused by Pine Wilt Disease: Platforms, Methods, and Future Directions. *Forests* **2024**, *15*, 2147. https://doi.org/10.3390/f15122147

Academic Editor: Isabel Pôças

Received: 2 November 2024
Revised: 23 November 2024
Accepted: 3 December 2024
Published: 5 December 2024
Corrected: 18 February 2025

1. Introduction

Pine wilt disease (PWD) is caused by the pine wood nematode (PWN, *Bursaphelenchus xylophilus*) and is transmitted by insect vectors such as *Monochamus alternatus*. Figure 1 illustrates *Monochamus alternatus* and PWN. It is a formidable forest disease and ranks among the most destructive and threatening pathogens in global forest ecosystems. It is characterized by an exceptionally high fatality rate, rapid progression, and significant ecological impact. This disease is a major concern for forestry and conservation worldwide [1–4]. Due to its high fatality rate, rapid onset, and challenging management, pine wilt disease has been metaphorically referred to as the "cancer" of pine trees [5,6].

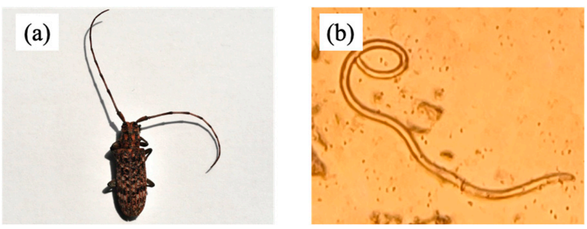

Figure 1. (**a**) *Monochamus alternatus* and (**b**) PWN under an optical microscope.

Figure 2 illustrates the distribution of PWD in major countries around the world. PWD is native to North America but has gradually spread to several countries in Asia and Europe since the 20th century [7]. Currently, the countries affected by PWD include China, Japan, South Korea, Mexico, France, Portugal, and Spain [8–10]. The widespread dissemination of this disease poses significant challenges to forest health and management worldwide [7,11–13]. Figure 3 illustrates the pine forest following infection by PWD, with the needle color of the pine trees transitioning from green to yellow and reddish-brown. Owing to the significant threat of PWD to forest ecosystems, the timely and accurate detection of infected pine trees and the exploration of an early identification window for discoloration caused by PWD are crucial for curbing the spread of the epidemic.

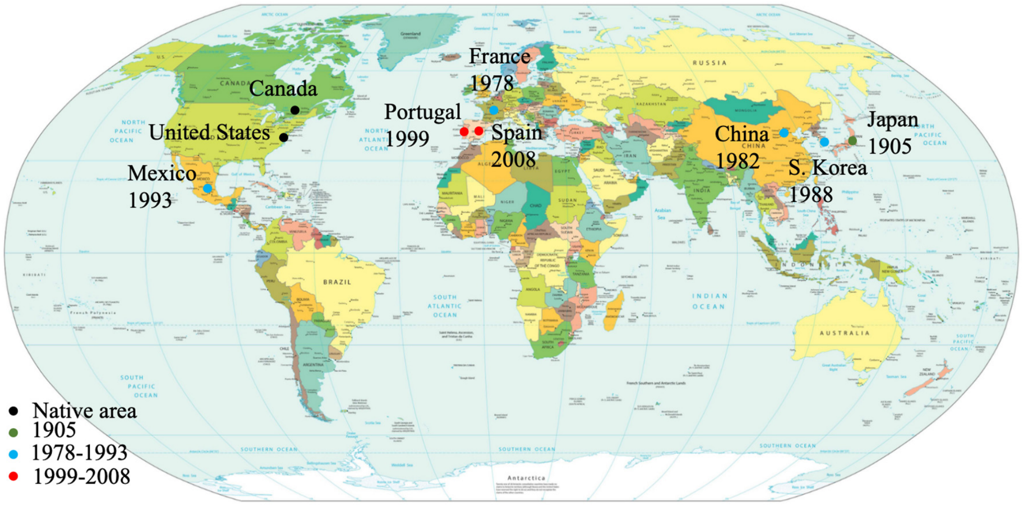

Figure 2. Global distribution map and first record timeline of pine wilt disease (the data are from https://www.cabidigitallibrary.org/doi/10.1079/cabicompendium.10448, accessed on 21 May 2024). Black represents the native countries of PWD, while green, blue, and red represent the countries where PWD has been introduced.

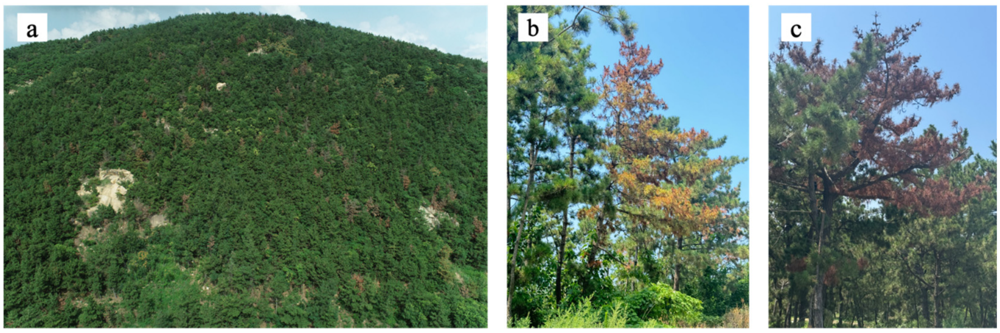

Figure 3. Pine forests affected by PWD. (**a**) represents the forest affected by PWD from a drone's perspective, and (**b**,**c**) are typical pine trees after infection.

Currently, the monitoring methods for discolored trees mainly involve ground surveys and remote sensing [14–16]. The ground survey includes discovering discolored pine trees, sampling and identifying pine wood nematodes, and identifying newly discovered epidemic pine forest patches [17]. These methods play a vital role in identifying and tracking the spread of the disease and facilitating effective management and control strategies. However, these approaches are constrained by environmental factors and may have relatively limited effectiveness. In the late 20th century, scholars began to apply satellite remote sensing to forest disease monitoring. They observed significant changes in some factors such as the transpiration rates, spectral characteristics, and vegetation indices after pine trees were infected [10,18,19]. Satellite remote sensing, which has wide coverage and low cost, is mainly used for large-scale monitoring [20–22]. Recently, with the continuous advancement of unmanned aerial vehicle (UAV) remote sensing, it has become increasingly feasible to acquire high spatial and temporal resolution remote sensing images rapidly and efficiently. UAVs can be equipped with various types of sensors to enhance their mobility and flexibility, allowing the real-time monitoring of forest disease outbreaks [23].

Traditional machine-learning methods have played a crucial role in identifying discolored wood using remote sensing images. Researchers manually select appropriate features and use classifiers for object recognition [24]. However, this approach mostly relies on domain expertise and experience and may not perform satisfactorily in situations where numerous ground objects exhibit similar color and morphological features as discolored trees. With the rise of deep-learning techniques, particularly convolutional neural networks (CNNs) [25], image processing has experienced a revolutionary breakthrough. Deep-learning methods enable the automatic learning of image features through neural networks, eliminate the need for manual feature selection, and significantly enhance the accuracy and efficiency of image recognition. In forest disease monitoring, deep-learning methods can effectively identify anomalies such as discolored trees and provide crucial support for the rapid detection and management of epidemics [26–32].

In recent years, several reviews on the detection of PWD have been published, with some [33–35] briefly discussing the overall research status and development trends of the remote sensing identification of PWD-discolored trees in a small section, while others [15] focus on the application of hyperspectral technology in the early detection of PWD, with few offering a comprehensive review. With the rapid advancement of computer technology, it is necessary to explore the advanced detection technologies, analyze potential methods that could enhance the detection accuracy of PWD-discolored trees, and provide significant references for the prevention and control of PWD. Consequently, this review extensively explores the remote sensing monitoring technologies for PWD-discolored trees, uncovers existing issues in the monitoring of PWD-discolored trees, and analyzes the impact of remote sensing monitoring platforms and identification methods on the detection accuracy of PWD-discolored trees. The collaborative use of multi-sensor systems and the early detection of PWD-discolored trees represent future development trends and research directions, aiming to provide a scientific foundation for more effective monitoring and management of PWD-discolored trees.

2. Introduction of PWD

2.1. Symptoms of Pine Trees After Infection with PWD

The PWN enters the interior of pine trees through branch wounds created by pine sawyer beetles and moves vertically or horizontally through resin channels, wood rays, and tracheids in the xylem [36]. With the rapid propagation of PWN, the duct is blocked. This leads to the gradual discoloration and withering of the pine needles, eventually turning reddish brown. Within a few months, the lack of water causes the pine tree to wither and die. The entire pine forest can succumb to PWD and perish within three to five years from the onset of infection by the PWN [37–39]. Pine trees exhibit both internal and external symptoms after infection. Internal symptoms refer to changes in physiological indicators within the pine tree that can be obtained using instruments or methods. External symptoms include observable changes in morphology, color, and texture characteristics. During the initial stages of PWD infection, changes in the internal physiological features are more apparent than changes in the external characteristics. The main internal physiological changes include a decrease in pine needle water content, chlorophyll, carotenoids, and transpiration rates [40–42].

Figure 4 shows drone images of pine trees at different stages of infection. From the figure, it can be seen that during the early stage, there are no apparent changes in external symptoms. As the disease progresses and deepens, changes in external features become evident. These changes primarily manifest as signs of pine sawyer beetle activity on the trunk and the discoloration and withering of pine needles [43]. After infection with PWD, the health status of pine trees generally goes through four stages until they reach a dead state [44,45]:

(1) Healthy Stage: The pine tree has a normal green color, and the resin secretion is normal. The trunks and branches have not been damaged by the pine sawyer beetles. The physiological metabolism and internal nutrient supply of the entire pine tree are normal.
(2) Green Attack Stage: The needles still appear green. However, resin secretion is normal or reduced, traces of beetle feeding can be found on tender branches, and PWN has already entered the pine tree.
(3) Early-Infection Stage: Some pine needles in the crown of the pine tree begin to change to slightly yellow or yellow–green. Resin secretion gradually decreases or even stops. At this stage, the signs of beetle oviposition and gallery formation are observed on the trunk.
(4) Mid-Infection Stage: Most needles of infected pine trees turn yellow–brown, and the pine trees exhibit wilting. The difference between the infected and healthy pine trees becomes apparent.
(5) Late-Infection Stage: Needles are reddish-brown, and the pine tree is completely dead and withered. The top needles droop but do not fall off.

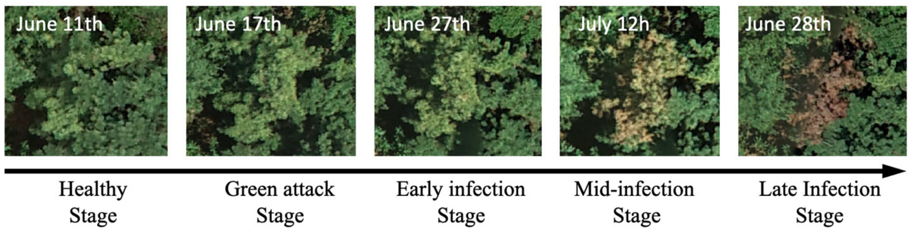

Figure 4. UVA images of pine trees at different stages of infection.

Based on the infection cycle pattern, the prevention and control of pine wilt disease mainly include the removal of epidemic trees, vector insect control, and trunk injection [46–48]. For infected and dead pine trees, the pine beetles on their trunks emerge only in the second year [49]. Therefore, autumn and winter are crucial for the removal of pandemic trees. Vector insect control involves spraying insecticides during the emergence period of beetles to kill the adult beetles [50]. Trunk injection treatment is conducted during the non-growing season (winter) of pine trees, which is used for both preventive and curative purposes against pine tree diseases [51].

2.2. The Theoretical Basis of Remote Sensing Identification for PWD

Remote sensing technology offers the surface information of the Earth through non-contact methods using remote sensors. In recent years, remote sensing has wide applications such as crop yield estimation, stress monitoring, and pest and disease detection [52–59]. The green (510–530 nm), red-edge (680–760 nm), and short-wave infrared (1400–1420 and 1925–1965 nm) bands are feasible for detecting the stress symptoms in Japanese and Korean pine trees. Kim et al. [60] measured the spectral reflectance of discolored and healthy trees 15 times from May to October. The reflectance of the red (600–700 nm) and near-infrared (1460–1550 nm) bands also increases. Healthy pine trees and pine trees infected with PWD exhibit distinct spectral features, providing potential possibilities for remote sensing in disease monitoring [61–64]. Figure 5 shows the spectral reflectance curves of the pine tree crowns at different stages of infection [65]. In a healthy state, pine needles typically exhibit high reflectance in the green wavelength range. As the infection by PWD intensifies, the needles begin to lose water and undergo physiological changes, leading to distinct alterations in spectral reflectance characteristics. Specifically, as the needles progressively wither and turn yellow, the red valleys and green peaks in the spectral curves gradually diminish, eventually flattening out in the visible light region to form an approximate straight line. This change reflects a decrease in chlorophyll content and a weakening of chlorophyll fluorescence. In the near-infrared region, the destruction of the internal structure of the needles, particularly the damage to mesophyll cells, results in a gradual decrease in reflectance. These changes in spectral characteristics provide crucial physiological and biochemical indicators for monitoring the progression of PWD.

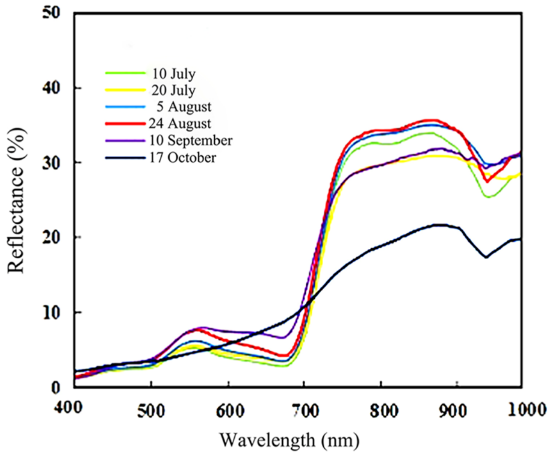

Figure 5. The spectral reflectance curves of infected trees at different infection stages [65].

3. Current Research Status of Remote Sensing Identification of PWD-Discolored Trees

3.1. Satellite-Based Identification of PWD-Discolored Trees

The distribution of discolored trees is generally scattered, often exhibiting individual spatial distribution [66]. Therefore, higher spatial resolution is required for satellite remote sensing imagery. Typically, it should be smaller than the diameter of a pine tree canopy, achieving meter- or sub-meter-level spatial resolution. Table 1 displays the fundamental parameters of the frequently employed satellite remote sensing data sources for monitoring forest diseases. It also provides information on the methods and precision in identifying forest pests and diseases.

Table 1. Fundamental parameters of satellite remote sensing data for recognition of discolored trees.

Sensor	Panchromatic/Multi-Spectral Images (m)	Revisit Period (day)	Classification Method	Overall Accuracy (%)	Reference
Landsat TM/TM+	30	16–18	Maximum likelihood Decision rule classifier Random forest	73 67–78 81.67	[67] [16] [68]
SPOT-5	2.5/10	2–3	Logistic regression	71	[69]
Quick Bird	0.61/2.44	4–7	Maximum likelihood Neural network	91 82.15	[70] [71]
IKONOS	1/4	1.5–3	ISODATA Maximum likelihood	71–91 68.18	[72] [73]
PlanetScope	3	1	Spatiotemporal detection	84.7	[19]
WorldView-2	0.5/2	1–4	Quadratic classifier Random forest	97.91–98.43 91.72	[74] [75]
GeoEye-1	0.5/1.65	1–3	Maximum likelihood	1.7 (error)	[22]
Sentinel-2	30	5	YOLOv5	74	[76]
BJ-2	0.8/3.2	1–2	CNN	99.4	[77]
GF-1	2/8	4	Residual network	87	[78]
GF-1 & GF-2	2/8 & 1/4	4–5	D-CNNs	94.90	[79]

As shown in Table 1, Landsat TM/ETM+ [16,67–69,80] is an early satellite remote-sensing sensor used to identify discolored trees. As its spatial resolution is only 30 m, it can only achieve forest-level monitoring of discolored trees. Furthermore, in mixed forests or sparse pine forests, there is often the issue of mixed pixels, leading to a monitoring precision of approximately 70%. With advancements in satellite remote sensing, high spatial resolution satellites, including WorldView-2 [75], GeoEye-1 [22], GF-1 [78], GF-2 [79], and BJ-2 [77], have been widely used, which enables the monitoring of forest diseases at the individual tree level. From Table 1, it is apparent that as the spatial resolution increases, the recognition precision improves. Additionally, researchers have achieved a precision of over 85% in identifying discolored trees using neural networks [77–79]. Although satellite remote sensing provides an effective means for large-scale monitoring of PWD, it is still influenced by factors such as spatial resolution, weather conditions, and revisit period, which imposes certain limitations on effective monitoring [20–22]. Additionally, many pine forests in China are mixed forests. In autumn, the color change and shedding of broad-leaved trees may affect the recognition results. Therefore, remote sensing images must be acquired during a window period when broad-leaved trees do not change their color.

3.2. PWD-Discolored Trees Using Unmanned Aerial Vehicle (UAV)

UAVs, such as remotely controlled unmanned aircraft, offer higher spatial resolution, provide more flexible operation, and are less affected by weather conditions than satellite remote sensing [81–84]. This has made UAVs an increasingly popular tool for forest disease monitoring, providing scientists and decision-makers with timely information to effectively control the spread of the disease. Table 2 summarizes the current progress in UAV remote sensing for the identification of discolored trees. RGB and multispectral data sources are widely used for identifying discolored trees because of their cost-effectiveness. Hyperspectral data sources with more spectral information, although more expensive, have greater potential for the early recognition of discolored trees and have been considered by researchers [15,85,86]. Both machine-learning and deep-learning methods can be used to process discolored tree images obtained by UAV, thereby attaining satisfactory recognition effectiveness [31,87,88].

Currently, both satellite and UAV remote sensing have been widely applied to monitor discolored trees caused by PWD [15,17,75–79]. Satellite remote sensing, which has extensive coverage and periodic observation capabilities, allows for large-scale monitoring of disease occurrence and estimates infected areas. However, in the early stages of infection and when the number of infected trees in a single pixel is low, the spectral information contained within a single pixel is relatively complex, and the spectral contribution of infected trees may be masked by the signal from healthy trees. Furthermore, the uneven distribution of trees in sparse pine forests further increases the complexity of spectral information. These factors collectively make it extremely challenging to accurately extract information about infected trees from satellite remote sensing data. As one of the latest technological approaches, UAV remote sensing has garnered widespread attention because of its high spatial and temporal resolutions and increased operational flexibility [89]. It dominates the remote sensing monitoring of discolored trees. Drones equipped with RGB, multispectral, hyperspectral, and LiDAR sensors can monitor forest diseases under complex terrain conditions. They can overcome the limitations of satellite remote sensing and achieve more accurate identification of discolored trees at the individual plant level. Drones can capture more detailed changes in infected pine trees and target specific areas for monitoring. For instance, studies [30,88,90,91] have achieved over 80% accuracy on RGB and multispectral datasets and approximately 90% overall accuracy on hyperspectral data [92–94]. Hyperspectral data, due to the advantage of its numerous bands, have certain advantages over other datasets, but they also face issues such as large data volume and the need for substantial computing resources for processing. Therefore, the absence of either remote sensing monitoring platform is indispensable. They complement each other and provide researchers with multidimensional and multi-scale data. This study provides a comprehensive and accurate foundation for monitoring PWD. Additionally, these data will assist in formulating more effective prevention and control measures and in protecting forest ecosystems.

Table 2. Unmanned aerial vehicle (UAV) remote sensing data sources for identifying discolored pine trees.

Data Source	Spatial Resolution (cm)	Method	Overall Accuracy (%)	Reference
RGB	10	HSV Thresholding	58–65	[95]
	8.47	Faster R-CNN AleNet, GoogeLeNet	82.42 65–80	[31] [32]
	8	U-Net	95.17	[30]
	6	YOLOv4	80.85	[96]
	8	DeepLabv3+	72–83.2	[27]
	4	Yolov8	81	[90]
	3.2–10.2	FPN	89.44	[97]
	10	MSSCN YOLOv3 Unsupervised method YOLOV5	89–94 94.39 91.35 89.05	[29] [98] [99] [100]
	5	DDNet	91.5	[101]
Multispectral	15	SCANet	79.33	[102]
	5	RF	95	[103]
	8	Multi-channel CNN	86.63	[91]
	1.59	RF, SVM, LDA	>80	[45]
	20–150	YOLOv5	86.8–88.5	[88]
	9	K-Nearest Neighbor	74.7–90	[104]
	--	YOLOv5	98.7	[105]
Hyperspectral	44	3D CNN	88.11	[92]
	40	RF RF	74.38 75–95	[106] [93]
	11	3D CNN	>90	[94]
	5.7	Mask R-CNN	83.51	[107]
	10	RF GA-SVM	91 95.24	[103] [108]
	2–12	RF	72.05–99.28	[65]

4. Main Identification Methods

4.1. Traditional Machine-Learning Classification Methods

Traditional machine-learning classification processes involve two key steps. (1) The extraction of image features because appropriate image features play a crucial role in the subsequent image classification. (2) The selection of a classifier to categorize the extracted image features effectively and display the classification results intuitively. The effective combination of these two steps is of great significance for the accuracy and performance of image classification and forms a critical link in traditional machine-learning classification methods.

4.1.1. Extracting Image Features

The identification of discolored trees primarily involves the extraction of color, texture, and morphological features from RGB images [30,109]. Tao et al. [95] proposed an HSV threshold image segmentation method, which distinguishes discolored trees from other objects in the "H-V space" and exhibits more pronounced clustering compared to the "G-R space". Zhang et al. [30] found that adding Haralick texture features to image data features reduced salt-and-pepper noise in the results. Liu et al. [109] mapped color and transparent texture features to form a new set of features.

The features extracted from multispectral and hyperspectral images typically include spectral features and vegetation indices. The spectral features of vegetation are relatively unique, with absorption troughs in the RGB wavelength range and reflection peaks in the near-infrared wavelength range [110]. The primary spectral features comprise red-edge position (REP), red-edge slope (RES), red band position (RBP), green peak height (GPH), and others [108]. Vegetation indices serve as simple and effective parameters for quantifying vegetation coverage and growth conditions; they have extensive applications in remote sensing and provide valuable insights into the physiological and physical parameters of vegetation [111]. The commonly used vegetation indices are summarized in Tables 3 and 4.

Table 3. Currently used multispectral vegetation indices.

Index Name	Formula	References
Normalized difference vegetation index (NDVI)	$\frac{NIR-Red}{NIR+Red}$	[112]
Green normalized difference vegetation index (GNDVI)	$\frac{NIR-Green}{NIR+Green}$	[113]
Difference vegetation index (DVI)	$NIR - Red$	[114]
Ratio vegetation index (RVI)	$\frac{NIR}{Red}$	[115]
Normalized difference red-edge index (NDRE)	$\frac{NIR-Red\ Edge}{NIR+Red\ Edge}$	[116]
Vegetation atmospherically resistant index (VARI)	$\frac{Green-Red}{Green+Red-Blue}$	[117]
Vegetation index green (VIgreen)	$\frac{Green-Red}{Green+Red}$	[117]
Normalized wilt index (NWI)	$NWI = -NDGI \times (NDVI + NDGI)$ $NDGI = \frac{Red-Green}{Red+Green}$	[118]
Plant senescence reflectance index (PSRI)	$\frac{Red-Blue}{Red\ Edge}$	[119]
Leaf chlorophyll index (LCI)	$\frac{NIR-Red\ Edge}{NIR+Red}$	[120]
Plant biochemical index (PBI)	$\frac{NIR}{Green}$	[121]

Note: Blue, Green, Red, Red Edge, and NIR represent the reflectivity of the blue band, green band, red band, red-edge band, and near-infrared band, respectively.

For the vegetation indices shown in Tables 3 and 4, single or combined vegetation indices can be used to identify PWD-discolored trees. For example, Skakun et al. [16] used the enhanced wetness difference index (EWDI) to classify discolored pine trees. Kim et al. [60] pointed out that the green–red spectral area index (GRSAI) is the optimal index for detecting discolored trees. Considering the poor classification performance of single vegetation indices, many studies have utilized combinations of different vegetation indices to identify the early and middle stages of PWD-discolored trees. Iordache et al. [103] selected 13 vegetation indices from numerous options to identify discolored trees. Yu et al. [106] employed a combination of vegetation indices, red-edge parameters, and moisture indices as input parameters for the random forest classifier to assess the stages of PWD infection. Zhang et al. [19] proposed a spatiotemporal change-detection method. They effectively distinguished ambiguous features by calculating the normalized green–red difference index (NGRDI) for two adjacent images with similar dates from different years. Compared with single-date image classification, this method significantly improved user's accuracy (81.2%

vs. 67.7%). Long et al. [68] combined five different long time-series vegetation indices to create the normalized difference forest index (NDFI). The effectiveness of the NDFI was verified using probability density curves. The combination of multiple vegetation indices as image data features reduces the potential errors associated with individual vegetation indices effectively. Additionally, constructing long time-series vegetation indices enables better classification of the “early-stage” disease.

Table 4. Currently used hyperspectral vegetation indices.

Index Name	Formula	References
Normalized difference vegetation index (NDVI)	$\mathrm{NDVI} = \frac{R_{800}-R_{670}}{R_{800}+R_{670}}$ $\mathrm{NDVI}(810,450) = \frac{R_{810}-R_{450}}{R_{810}+R_{450}}$	[122,123]
Green normalized difference vegetation index (GNDVI)	$\frac{R_{800}-R_{540}}{R_{800}+R_{540}}$	[113]
Red-edge normalized difference vegetation index (RENDVI)	$\frac{R_{750}-R_{705}}{R_{800}+R_{680}}$	[124]
Red-edge inflection point (REIP)	$700 + 40 \times \frac{(R_{670}+R_{820})/2-R_{700}}{R_{740}-R_{700}}$	[125]
Greenness index (GI)	$\frac{R_{554}}{R_{677}}$	[126]
Plant senescence reflectance index (PSRI)	$\frac{R_{677}-R_{500}}{R_{750}}$	[127]
Plant stress index (PSI)	$\frac{R_{695}}{R_{760}}$	[128]
Ratio vegetation stress index (RVSI)	$\frac{R_{600}}{R_{760}}$	[128]
Normalized difference water index (NDWI)	$\frac{R_{864}-R_{1245}}{R_{864}+R_{1245}}$	[129]
Photochemical reflectance index (PRI)	$\frac{R_{570}-R_{531}}{R_{570}+R_{531}}$	[130]
Moisture stress index (MSI)	$\frac{R_{1600}}{R_{820}}$	[131]

Several redundant spectral bands exist in hyperspectral remote sensing images, making the selection of appropriate spectral bands a crucial challenge in hyperspectral technology. Studies have found that using feature bands selected by genetic algorithms (GAs) [132,133] to build predictive models can improve the accuracy of PWD-discolored tree identification, thereby optimizing the feature selection problem in hyperspectral technology. Competitive adaptive reweighted sampling (CARS) [134] and the successive projections algorithm (SPA) [135] are also commonly used for band selection. The CARS algorithm simulates the concept of “survival of the fittest” through iterative statistical variable selection, adaptively adjusting the selection probabilities of each band, ultimately selecting the optimal band combination that contributes the most to modeling performance. The SPA, on the other hand, selects variable combinations that contain the least amount of redundant information and the lowest collinearity through vector projection analysis. Li et al. [136] used CARS and the SPA algorithm to select feature bands and obtained overall accuracies of 77% and 78% for the Japanese and Korean pine trees, respectively. Zhang et al. [137] extracted feature bands from high-resolution hyperspectral images through principal component analysis (PCA), the SPA, and the instability index between classes (ISIC). The average accuracy was 95.23%. Additionally, the use of a spectroradiometer combined with hyperspectral images can enhance the classification of healthy and infected pine trees [15,138]. Currently, feature band extraction is primarily accomplished using single or coupled multiple algorithms. However, this method has the limitation of manual feature selection and lacks strong generalization ability. To avoid excessive reliance on manual feature selection and improve the robustness of the algorithm, some researchers have proposed more automated methods. Among them, Wan et al. [99] proposed an unsupervised decision fusion method that combined adaptive thresholds and lab-space clustering to automatically extract feature bands.

4.1.2. Classic Supervised Classifier

Classic supervised classifiers require pre-labeled sample data to train the classifier. For the identification of discolored trees, commonly used classic supervised classifiers include maximum likelihood [22], logistic regression [69], neural networks [139], K-nearest neighbors [104], random forest [68], and support vector machine [108]. The random forest classifier is the most widely used classifier for detecting PWD-discolored trees [65,93,103,106]. Traditional machine-learning classifiers use pixel-level spectral data to classify images. But high spatial resolution images, like those from drones, do not have much spectral data. This makes it hard for these classifiers to do well in classifying and extracting details from such images. For example, there are issues such as lower classification accuracy, more noise, and suboptimal extraction results. Therefore, traditional machine-learning methods are currently mainly utilized in the task of identifying PWD-discolored trees in multispectral and hyperspectral images.

4.2. The Classification Method Based on Deep Learning

In recent years, with the advancement of computer and artificial intelligence technologies, various deep-learning methods have been widely applied in remote sensing. Deep-learning methods provide an automated method to learn features from the training dataset, replacing the traditional manual feature selection process. This method enables the learning of both shallow features and deep nonlinear features, resulting in a higher generalization capability. Convolutional neural networks (CNNs) [140], an early proposed algorithm for object recognition, consists of three layers: a convolutional layer, max pooling layer, and fully connected layer. Tao et al. [32] used AlexNet [141] and GoogLeNet [142] to identify discolored trees, achieving higher recognition accuracy than traditional template matching algorithms. Zhou et al. [78] compared five different depths of residual networks and found that ResNet18 exhibited the best recognition performance. However, traditional CNNs perform poorly in multi-class recognition tasks. To further improve the recognition performance, CNN-based object detection [143,144] and semantic segmentation [27,92,94] algorithms have been developed, which can realize more accurate recognition of single- or multi-class targets.

4.2.1. Recognizing Discolored Trees Using Object Detection Algorithms

Current dominant object detection algorithms can be divided into two categories: two-stage object detection algorithms based on candidate regions and one-stage object detection algorithms based on regression [145]. In the case of one-stage algorithms, the features are directly extracted using CNNs for object classification and localization. Two-stage algorithms involve candidate box generation and subsequent object classification and localization using CNNs. Compared to one-stage algorithms, two-stage algorithms generally achieve higher accuracy but have higher computational costs and slower classification speeds. The original object detection algorithms primarily focus on datasets, such as PASCAL VOC, ImageNet, and MS COCO [146], in which the object sizes are relatively large. However, the PWD-discolored areas of trees occupy a small proportion of pixels. Therefore, directly applying the original object detection algorithms results in poor performance in identifying discolored trees. To address this issue, researchers usually improve the networks to enhance the accuracy of PWD recognition. Table 5 presents the commonly used network models for the remote sensing recognition of PWD, along with their main contributions.

Table 5. Remote sensing studies on discolored trees detection using object recognition algorithms.

Network Type	Method	Main Contributions	Number of Classes	Early Stage	Overall Accuracy (%)	Recall (%)	Reference
Two-stage	Faster-RCNN	Modify anchor box sizes in region proposal network.	3	No	82.42	88.11	[31]
	Faster-RCNN	Replace Softmax loss with sigmoid loss, change anchor box sizes, and use ResNet101 instead of VGG16.	1	No	89.1	90	[147]
	Faster-RCNN	Incorporate test-time augmentation (TTA) and weighted box fusion (WBF) for increased test sample diversity and better predictions.	7	No	59.5	83.2	[97]
	R-CNN	Design a multi-channel feature extractor.	2	No	86.63	--	[91]
One-stage	YOLOv3	Replace backbone with EfficientNet-B1, add channel attention module, and use pyramid pooling module (PPM) in neck.	3	Yes	94.39	87.35	[98]
	YOLOv4	Using the lightweight learning network MobileNetv2 as the backbone for YOLOv4 and incorporating CBAM and Inceptionv2 structures.	1	No	86.85	91.58	[148]
	YOLOv5	A module combining CBAM and CA (Coordinate Attention) enhances feature extraction for small-scale pine nematode trees, while Transformer and BiFPN improve feature fusion.	1	No	98.7	97.3	[105]
	FCOS	Introduce global multiscale channel attention (GMCA) module into feature pyramid network (FPN).	2	No	79.8	86.6	[149]
	YOLOv5	Fuse four YOLOv5 variants, create a dual-branch network for RGB and multispectral image fusion, and use multi-head attention (MHA) mechanism with multiband feature fusion transformer (MFFT) module and feedforward neural network (FNN).	4	Yes	87.65	--	[88]
	EfficientNetv2-S	Create a virtual forest using 3D rendering tools to synthesize a dataset.	3	No	92.88	93.07	[150]

Faster R-CNN is a main two-stage object detection algorithm and has been widely applied to identify PWD-discolored trees, as shown in Table 5. Researchers have optimized various aspects of this algorithm, such as feature extraction networks, region proposal networks, and loss functions. To utilize the features from both RGB light and multispectral images effectively, Park et al. [91] designed a multi-channel feature extractor that can extract features from different types of images simultaneously. Additionally, some researchers replaced the VGG16 feature extraction network with a residual network (ResNet) to increase the network depth and improve the recognition accuracy while mitigating the vanishing gradient problem [151]. On the other hand, the traditional feature extraction network only extracts feature maps at the final convolutional layer and therefore does not fully utilize information from high spatial resolution images. To address this issue, You et al. [97] employed a feature pyramid network (FPN) to extract multi-scale features from both top-down and bottom-up pathways. They fused shallow high-resolution image features with deep semantic features, enhancing the prediction capability of the network. For the region proposal network, the original anchor box sizes are relatively large and unsuitable for the recognition and localization of discolored trees. Therefore, researchers have modified the sizes of the anchor boxes (an auxiliary tool used to define the location and size of targets) to enhance the identification of discolored trees [31,147]. Deng et al. [147] treated the discolored tree recognition problem as a binary classification problem and replaced the Softmax function with the Sigmoid function, which improved the calculation of the gap between the actual and predicted values. Furthermore, some researchers have proposed a weakly supervised deep-learning network [152] that requires only images containing discolored trees as positive training samples and images without discolored trees as negative training samples. This approach uses class activation maps to localize the target and significantly reduces the effort required for sample labeling.

For the recognition of discolored trees, the one-stage object detection algorithm is mainly represented by the YOLO series of algorithms. Researchers have optimized the backbone networks, feature pyramids, and loss functions to improve identification precision. For the variants of YOLOv5, Zhou et al. [88] proposed a mid-level fusion mode using a dual-branch network to simultaneously fuse RGB light and multispectral image features. In other studies, the original backbone networks of YOLO series algorithms were replaced with other networks, such as EfficientNet-B1 and MobileNetv2 [98,148], which exhibit better performance and faster recognition speeds. Li et al. [66] introduced a bidirectional feature pyramid network (BiFPN) to replace YOLOv5's pyramid network (PANET). The BiFPN achieves rapid multi-scale feature fusion, enhancing foreground features from the top down and background features from the bottom up, thereby achieving better detection results. Adding attention modules to the feature pyramid is another common method for network improvement [88,149]. This allows the model to focus on discolored trees, suppress irrelevant information from non-target areas, reduce the interference of complex environments in feature extraction, and effectively improve the accuracy of PWD detection. Ye et al. [143] combined YOLOv5 with StrongSORT (Strong Simple Online Real-Time Tracking) to achieve the dynamic visual tracking and counting of PWD-infected trees. Currently, most object detection models rely on predefined anchor boxes or proposal regions. To address this issue, Ren et al. [149] proposed a fully convolutional one-stage object detector (FCOS), which adopts pixel-wise prediction for PWD recognition. FCOS achieves anchor-free and proposal-free object detection, reduces computational overhead and hyperparameter design, improves training speed, and enhances detection accuracy.

4.2.2. Recognizing Discolored Trees Using Semantic Segmentation Algorithms

Target detection algorithms for the identification of PWD can generate bounding boxes and positional information of discolored trees. However, these methods may not provide specific sizes and morphological information of the affected regions, which are crucial for determining the extent of PWD infection. To address this issue, researchers have adopted semantic segmentation networks to achieve the precise recognition of affected areas. Zhang et al. [30] used the U-Net segmentation network for the identification and segmentation of early discolored trees. The results were compared with those of the random forest algorithm and found that the U-Net instance segmentation algorithm outperformed the RF algorithm, providing higher recognition accuracy. More researchers have then sought to improve the segmentation network model to enhance the identification performance of PWD. The methods used to improve the model are listed in Table 6.

For semantic segmentation networks, the addition of attention modules is a common method for network improvement. Li et al. [94] addressed the problem of expensive instance segmentation labeling costs by introducing a one-class method (OCC) that focused only on the PWD category, effectively reducing the workload of labeled samples. To solve the issue of imbalanced PWD sample data in the testing set when using OCC, they proposed a balanced, unbiased detection risk estimator and constructed a detector based on OCC and 3D convolutional layers with transformation blocks. Han et al. [29] also tackled the problem of the imbalanced distribution of discolored tree samples in the data by employing an adaptive oversampling (copying samples from minority classes or generating new samples) and allocation method to augment the samples. Wang et al. [153] trained DeepLabv3+, HRNET, and DANET and selected HRNET as the generator based on the experimental results to construct a GAN-based semi-supervised semantic segmentation model. This model reduces the laborious task of building a training dataset and improves the generalization performance of the model by extracting features from a small amount of labeled data and a large amount of unlabeled data.

Table 5 shows that (1) the performance of the improved one-stage object detection algorithms is superior to that of the two-stage algorithms. (2) As the number of classes in the dataset increases, there is a varying degree of decline in overall accuracy and recall. (3) When identifying pine trees in the early stages, the model's performance experiences a certain degree of decline. Currently, with the updates to one-stage algorithms, one-stage algorithms not only have better performance but also possess a faster detection speed. As the number of classes in the dataset increases, the model needs to process more class information, which may lead to increased model complexity and thus affect overall recognition performance. In the early stages, the external characteristics of diseased trees may be subtle and difficult to distinguish clearly through remote sensing images. Additionally, the spectral features of early-stage disease may not differ significantly from those of healthy trees, making it challenging for models to capture these subtle changes, thereby affecting recognition performance. Comparing Tables 5 and 6, it can be concluded that (1) segmentation algorithms generally have lower overall accuracy and recall than object recognition algorithms. (2) Using hyperspectral data for identifying PWD-discolored trees can significantly improve model performance.

Current research on the improved algorithms for the detection and segmentation of PWD mainly focuses on recognition models, network structures, and data augmentation.

Regarding recognition models, researchers have advanced from strong supervision to weak- and semi-supervised models, achieving more intelligent recognition approaches [152,153]. Strongly supervised models require a large number of labeled samples but can achieve higher accuracy. In contrast, weakly supervised and semi-supervised models learn from fewer labeled or unlabeled samples, thus reducing the workload of labeling samples. These novel supervised learning methods provide flexible and efficient solutions for PWD recognition.

Table 6. Remote sensing identification studies of discolored trees using semantic segmentation algorithms.

Method	Improvement	Number of Classes	Early Stage	Overall Accuracy (%)	Recall (%)	Reference
ASCANet	Comprising space information preservation module (SIRM) and context information module (CIM) and incorporating attention enhancement module (ARM).	2	No	79	91	[102]
DeepLabv3+	Using Resnet as the backbone, enhancing boundary acquisition through the decoder–encoder structure built on top of Atrous Spatial Pyramid Pooling (ASPP).	2	No	83.8	82.6	[27]
3D-CNN	Integrating residual modules into the three-dimensional convolutional neural network (3D-CNN).	3	Yes	88.11	88.04	[92]
3D-CNN	Utilizing one-classification as the fundamental principle of the framework, proposing balanced unbiased detection risk estimator, and constructing OCC-based 3D convolutional layers and transformation blocks for the detection model, focusing on discriminative regions using the attention module.	1	No	92.06	82.97	[94]
CNN	Adding multi-scale spatial attention module to the fully convolutional neural network, and using copy-paste augmentation strategy to augment the effective dataset.	2	No	94	84	[29]
U-Net	Introducing multi-scale convolution, adaptive pooling, and attention module into U-Net.	3	No	57.9	57.38	[154]
GAN	Selecting HRNET model as the generator for GAN and constructing a GAN-based semi-supervised semantic segmentation model.	2	No	69.61	80.09	[153]

In terms of network structure, improvements include optimizing the network architecture, incorporating attention mechanisms, and using lightweight networks. Optimizing the network structure aims to enhance the learning and generalization capabilities of the model, thereby improving the recognition accuracy [66,155]. The introduction of attention mechanisms allows the network to focus more on important image regions, thereby reducing excessive reliance on irrelevant information [102,143,154]. Lightweight networks can maintain certain performance while reducing computational complexity, thereby increasing detection speed [98,105,148].

Data augmentation is another essential improvement direction. Traditional data augmentation methods include geometric, color, and mix-up transformations, which increase the diversity of the training data and improve the robustness of the model [147,151]. Additionally, generating new data is an effective data augmentation method [150,153]. Creating synthetic samples can increase the quantity and quality of training data, thereby enhancing model performance.

Based on the analysis of the current research status, the following conclusions can be drawn: First, machine-learning and deep-learning methods currently coexist in the research on identifying discolored trees. Second, deep learning has been increasingly applied to the identification of discolored trees. Finally, researchers have focused more on the early stages. Currently, deep-learning methods are more commonly applied in RGB images, whereas machine-learning algorithms are more commonly applied in multispectral and hyperspectral images.

5. Problems in Current Research

5.1. Challenges of Remote Sensing Platforms in Monitoring PWD-Discolored Trees

In monitoring pine tree discoloration caused by PWD, both the satellite and UAV remote sensing platforms have advantages and limitations. In recent years, satellites with sub-meter level spatial resolutions have been launched, which can meet the high-precision monitoring requirements for individual discolored trees. Although satellite remote sensing can only identify the later stages of discoloration, it provides convenience for monitoring widespread areas of diseased trees [16,67,69,80]. UAVs, which are low-altitude flying devices, can capture high spatial- and temporal-resolution images, aiding in the detailed observation of specific regions affected by discoloration. The flexible operational capabilities of UAVs allow for the adjustment of flight paths based on practical requirements, thereby providing support for targeted monitoring. UAVs can carry sensors such as hyperspectral and LiDAR; however, the high cost of these devices may limit their widespread application. Additionally, UAVs face constraints related to data storage, airspace regulations, and endurance [15].

Currently, remote sensing monitoring of PWD focuses on the discoloration phenomenon. Using only remote sensing imagery to identify PWD may lead to misjudgments. Potential reasons must be combined with ground surveys, field investigations, and sampling to determine the existence of PWD in the area. Additionally, due to the extremely high mortality rate of PWD (often resulting in the death of pine trees within a few months), manual surveys are subject to delays. If large areas of discolored trees are found in remote sensing images, they are most likely caused by PWD. Therefore, remote sensing monitoring of PWD is of great significance. Furthermore, climate change can lead to the discoloration of broad-leaf trees, grasslands, sparse vegetation, exposed rocks, and shadows between trees, thereby affecting the identification accuracy. Some researchers have included objects resembling "similar diseases" in the training dataset to enhance the detection of PWD-discolored trees [26,97]. Determining whether discolored trees are infested with PWD is crucial for taking appropriate measures to protect pine forests.

5.2. The Impact of the Classification Method on the Identification of PWD-Discolored Trees

Currently, both traditional machine-learning and deep-learning methods are applied to identify discolored trees. Traditional machine-learning methods are relatively simple and have low sample requirements, especially when vegetation indices are used to identify discolored trees, thereby enabling the study of their physiological and physical parameters. However, traditional methods may not fully utilize the spatial information in high spatial and temporal resolution images. Deep-learning methods excel at automatically learning features rather than relying on manual feature selection and provide superior nonlinear fitting capabilities. However, deep learning typically requires numerous training samples. To reduce the requirement for the number of training samples, Wang et al. [153] proposed a semi-supervised learning model based on Generative Adversarial Networks (GANs), which combines a limited number of labeled samples with a large pool of unlabeled samples to reduce the workload of manual annotation while enhancing the model's generalization capabilities. In practical applications, a dataset was constructed using Gaofen-2 high-resolution remote sensing images, and the model achieved a recall rate of 80.09%. Addressing the issue of large data collection from drones, Li et al. [156] proposed an improved lightweight YOLOv4-Tiny method, which utilizes edge devices to filter out uninterested images for rapid preliminary detection. The remaining images are then transmitted to the ground workstation for fine-grained detection. Zhang et al. [44] indicated that random forest and three-dimensional convolutional neural networks (3D-CNNs) achieved comparable results in recognizing discolored trees. Deep learning has powerful learning capabilities; however, its full potential has not yet been realized.

Additionally, the overall accuracy and recall rates of semantic segmentation net-works are generally lower than those of object detection algorithms. This is because semantic segmentation networks aim to assign the correct class labels to every pixel in the image, which requires the model to understand more nuanced spatial relationships and contextual information. At present, many researchers are exploring the application of deep learning to identify PWD-discolored trees, such as multi-scale feature fusion, attention mechanisms, and semi-supervised and unsupervised learning. While deep-learning methods possess considerable power, we need to take a comprehensive consideration of practical applications. For instance, when dealing with multispectral and hyperspectral images, using vegetation indices as inputs for traditional machine-learning models can offer rapid detection speeds and decent accuracy. By contrast, when faced with high spatial resolution images, deep-learning algorithms can automatically learn hierarchical representations from raw data, achieving higher accuracy rates.

6. Potential Research Topics

6.1. Multi-Sensor Collaborative Identification of PWD-Discolored Trees

For the identification of discolored trees, the most commonly used sensors are RGB, multispectral, and hyperspectral. Current research mainly relies on a single sensor to identify PWD. However, some researchers have explored the impact of combining multiple sensors on recognition accuracy. However, a comprehensive assessment of their integrated performance is lacking and requires further research.

At present, multi-source data fusion is used to identify PWD-discolored trees, and it can be categorized into three types: data fusion between drones, data fusion between drones and satellites, and data fusion among satellites

Data fusion between drones is a method that involves integrating data from different drone platforms or drones equipped with various sensors. By combining the data from drones with high spatial resolution imaging capabilities and those from drones equipped with multispectral, hyperspectral, LiDAR, or thermal imaging sensors, a more comprehensive assessment of forest health can be achieved and the identification accuracy of PWD-discolored trees can be enhanced. For example, Zhou et al. [88] proposed a deep-learning-based multi-band fusion detector that can extract features from RGB and multispectral images. This method can enhance the information correlation between the two types of data, achieving higher recognition accuracy (9.2%) than a single sensor. Yu et al. [157] combined LiDAR with hyperspectral data and achieved a 7.1% increase in detection and recognition accuracy compared to using only a hyperspectral sensor. Zhang et al. [44] demonstrated that the addition of a long-wave infrared band to multispectral sensors can effectively improve recognition accuracy (9.47%).

When it comes to data fusion between drones and satellites, drones can provide high-resolution local images, while satellites can cover broader areas. By integrating these two types of data sources, it is possible to monitor forest conditions on a large scale while using drone data for a more detailed analysis of specific areas. Li et al. [66] integrated UAV and 8 m resolution Radarsat-2 satellite imagery, expanding the training samples of 30 m resolution Sentinel-1 through a two-stage up-sampling strategy. By applying a random forest algorithm, they achieved a detection of PWD infection at medium and high levels across various scales, with a classification accuracy of 87.63% for Sentinel-1 and 72.57% for Radarsat-2.

In practical applications, the use of drones equipped with edge-computing devices to process and analyze data near the data source can reduce data transmission latency, which makes real-time monitoring and rapid response possible [88,156]. This is particularly important for forest pest and disease management scenarios that require immediate decision-making. Regarding the issue of how multi-source data can collaborate in training, federated learning provides a method for collaborative model training among multiple data holders without the need to centralize data. This approach can protect data privacy while leveraging dispersed data sources to improve the model's accuracy and generalization ability in identifying PWD-discolored trees. Through federated learning, a powerful model can be constructed that integrates drone and satellite data from different regions and conditions to enhance the identification accuracy of different PWD infection stages.

6.2. Early Monitoring of PWD-Discolored Trees

Currently, most studies focus on single-date images to effectively identify visibly discolored PWD-infected pine trees. However, the complete temporal dynamics of PWD have not been explored, and the ability to control the epidemic at an early stage is lacking. The definition of "early" PWD monitoring remains unclear, with most studies defining it as the slight discoloration of pine tree crowns. However, in the green attack stage, pine trees are already affected by pine wood nematodes before discoloration. Hyperspectral sensors are more sensitive to changes in the water content of pine needles because of their ability to extract continuous spectral information from pine tree crowns [136]. This provides the possibility for true "early-stage" monitoring. Researchers have explored spectral feature changes and identification windows by collecting time-series images of infected crowns. However, the collection frequency of long-time series images is generally low, with intervals ranging from 10 days to two months, lacking short-interval long-time sequence image data [45,93,103]. Short-interval image data collection is beneficial for better observing the dynamic changes in PWD, providing data support for selecting optimal spectral features and refining the monitoring window period. This is significant for achieving the fine-grained monitoring and control of PWD.

Future research should focus on improving the accuracy of PWD-discolored tree identification at various stages. This can be achieved by increasing the data collection frequency and evaluating the multi-sensor fusion systems systematically. For early monitoring, current studies rely mainly on single-date images, which cannot be used to explore the complete temporal dynamics of PWD. Hyperspectral sensors show promise for true "early-stage" monitoring. Therefore, short-interval and long-time sequence image data are crucial for fine-grained monitoring and control. There is an urgent need to monitor, recover, and manage pine forests following the detection of discolored trees. However, weather conditions can significantly impact the frequency and quality of data acquisition. In addition, there is a need for higher equipment costs, labor, and computational resources. Currently, regarding the issue of large data volumes in hyperspectral imagery, apart from dimensionality reduction, there are efficient compression methods based on Tensor-Based Compressive Sensing [158], Kronecker Compressive Sensing [159], and others for hyperspectral data. These methods aim to minimize data volume while ensuring quality, providing viable solutions for real-time or near-real-time monitoring.

7. Conclusions

In current research, remote sensing platforms face challenges in monitoring PWD-discolored trees. Satellite and UAV platforms each have their strengths and limitations. Satellite remote sensing is suitable for large-scale monitoring, while UAVs can provide high spatial and temporal resolution images, which aid in the detailed observation of specific areas. However, the use of UAVs is limited by cost, data storage, airspace regulations, and endurance capabilities. Currently, remote sensing monitoring primarily focuses on the discoloration phenomenon, but relying solely on remote sensing imagery may lead to misjudgments, and it is necessary to combine ground surveys to determine the presence of

PWD. When selecting classification methods, consideration should be given to real-world scenarios, especially when dealing with hyperspectral and multispectral data. Utilizing vegetation indices and traditional machine-learning approaches can quickly provide quantitative information on forest health status and enable the rapid and effective identification of forest diseases. In the face of high spatial resolution imagery, employing deep-learning algorithms can automatically learn hierarchical representations from raw data, achieving higher accuracy rates.

The future trends and research directions focus on the collaborative use of multiple sensors and the early identification of PWD-discolored trees. The core of this direction lies in leveraging the strengths of different sensors and enhancing the monitoring accuracy and timeliness of PWD-discolored trees through data fusion and algorithm optimization. Specifically, future research will explore ways to integrate data from satellites, UAVs, and other ground sensors to achieve the comprehensive monitoring of forest health status.

Author Contributions: Conceptualization, R.Z. and L.C.; methodology, R.Z. and H.S.; investigation, H.S.; resources, R.Z., M.C. and L.C.; writing—original draft preparation, H.S.; software, Q.W.; data curation, H.S. and D.Z.; writing—review and editing, H.S., R.Z. and M.C.; supervision, R.Z. and L.C.; project administration, R.Z., M.C. and L.C.; funding acquisition, R.Z. and M.C. All authors have read and agreed to the published version of the manuscript.

Funding: This work was funded by the National Key R&D Program of China (2021YFD1400900), the Promotion and Innovation of Beijing Academy of Agriculture and Forestry Sciences (KJCX20230205), and the National Natural Science Foundation of China (31971581).

Data Availability Statement: Not applicable.

Conflicts of Interest: The authors declare no conflicts of interest.

References

1. Fonseca, L.; dos Santos, M.C.V.; de A Santos, M.S.N.; Curtis, R.H.C.; de O Abrantes, I.M. Morpho-biometrical characterisation of Portuguese *Bursaphelenchus xylophilus* isolates with mucronate, digitate or round tailed females. *Phytopathol. Mediterr.* **2008**, *47*, 223–233.
2. Hunt, D. Pine wilt disease: A worldwide threat to forest ecosystems. *Nematology* **2009**, *11*, 315–316. [CrossRef]
3. Khan, M.A.; Ahmed, L.; Mandal, P.K.; Smith, R.; Haque, M. Modelling the dynamics of Pine Wilt Disease with asymptomatic carriers and optimal control. *Sci. Rep.* **2020**, *10*, 11412. [CrossRef] [PubMed]
4. Li, Y.X.; Zhang, X.Y. Analysis on the trend of invasion and expansion of *Bursaphelenchus xylophilus*. *For. Pest Dis.* **2018**, *37*, 1–4.
5. Carnegie, A.J.; Venn, T.; Lawson, S.; Nagel, M.; Wardlaw, T.; Cameron, N.; Last, I. An analysis of pest risk and potential economic impact of pine wilt disease to *Pinus* plantations in Australia. *Aust. For.* **2018**, *81*, 24–36. [CrossRef]
6. Kim, N.; Jeon, H.W.; Mannaa, M.; Jeong, S.I.; Kim, J.; Kim, J.; Lee, C.; Park, A.; Kim, J.C.; Seo, Y.S. Induction of resistance against pine wilt disease caused by *Bursaphelenchus xylophilus* using selected pine endophytic bacteria. *Plant Pathol.* **2019**, *68*, 434–444. [CrossRef]
7. Sutherland, J.R. A Brief Overview of the Pine Wood Nematode and Pine Wilt Disease in Canada and the United States. In *Pine Wilt Disease*; Zhao, B.G., Futai, K., Sutherland, J.R., Takeuchi, Y., Eds.; Springer: Tokyo, Japan, 2008; pp. 13–17.
8. Kim, B.-N.; Kim, J.H.; Ahn, J.-Y.; Kim, S.; Cho, B.-K.; Kim, Y.-H.; Min, J. A short review of the pinewood nematode, *Bursaphelenchus xylophilus*. *Toxicol. Environ. Health Sci.* **2020**, *12*, 297–304. [CrossRef]
9. de la Fuente, B.; Saura, S.; Beck, P.S.A. Predicting the spread of an invasive tree pest: The pine wood nematode in Southern Europe. *J. Appl. Ecol.* **2018**, *55*, 2374–2385. [CrossRef]
10. Zhang, Y.; Dian, Y.; Zhou, J.; Peng, S.; Hu, Y.; Hu, L.; Han, Z.; Fang, X.; Cui, H. Characterizing Spatial Patterns of Pine Wood Nematode Outbreaks in Subtropical Zone in China. *Remote Sens.* **2021**, *13*, 4682. [CrossRef]
11. Guo, D.; Zhao, B.; Gao, R. Experiments on the relationship between the bacterium isolate B619 and the pine wilt disease by using Calli of *Pinus thunbergii*. *J. Nanjing For. Univ. (Nat. Sci. Ed.)* **2001**, *5*, 71–74.
12. Mota, M.M.; Braasch, H.; Bravo, M.A.; Penas, A.C.; Burgermeister, W.; Metge, K.; Sousa, E. First report of *Bursaphelenchus xylophilus* in Portugal and in Europe. *Nematology* **1999**, *1*, 727–734. [CrossRef]
13. Abelleira, A.; Picoaga, A.; Mansilla, J.P.; Aguin, O. Detection of *Bursaphelenchus Xylophilus*, Causal Agent of Pine Wilt Disease on *Pinus pinaster* in Northwestern Spain. *Plant Dis.* **2011**, *95*, 776. [CrossRef] [PubMed]
14. Oumar, Z.; Mutanga, O. Using WorldView-2 bands and indices to predict bronze bug (*Thaumastocoris peregrinus*) damage in plantation forests. *Int. J. Remote Sens.* **2013**, *34*, 2236–2249. [CrossRef]
15. Wu, W.; Zhang, Z.; Zheng, L.; Han, C.; Wang, X.; Xu, J.; Wang, X. Research Progress on the Early Monitoring of Pine Wilt Disease Using Hyperspectral Techniques. *Sensors* **2020**, *20*, 3729. [CrossRef]

16. Skakun, R.S.; Wulder, M.A.; Franklin, S.E. Sensitivity of the thematic mapper enhanced wetness difference index to detect mountain pine beetle red-attack damage. *Remote Sens. Environ.* **2003**, *86*, 433–443. [CrossRef]
17. Lee, J.-P.; Sekhon, S.S.; Kim, J.H.; Kim, S.C.; Cho, B.-K.; Ahn, J.-Y.; Kim, Y.-H. The pine wood nematode *Bursaphelenchus xylophilus* and molecular diagnostic methods. *Mol. Cell. Toxicol.* **2021**, *17*, 1–13. [CrossRef]
18. Shimu, S.A.; Aktar, M.; Afjal, M.I.; Nitu, A.M.; Uddin, M.P.; Mamun, M.A. NDVI Based Change Detection in Sundarban Mangrove Forest Using Remote Sensing Data. In Proceedings of the 2019 4th International Conference on Electrical Information and Communication Technology (EICT), Khulna, Bangladesh, 20–22 December 2019; pp. 1–5.
19. Li, N.; Huo, L.; Zhang, X. Using only the red-edge bands is sufficient to detect tree stress: A case study on the early detection of PWD using hyperspectral drone images. *Comput. Electron. Agric.* **2024**, *217*, 108665. [CrossRef]
20. Tang, L.; Shao, G. Drone remote sensing for forestry research and practices. *J. For. Res.* **2015**, *26*, 791–797. [CrossRef]
21. Wang, L.; Zhang, X.; Luo, Y.; Shi, J.; Huang, H. A study on the changes of *Pinus massoniana* spatial pattern by pine wood nematode invasion based on remote sensing and GIS. In Proceedings of the 2006 IEEE International Symposium on Geoscience and Remote Sensing, Denver, CO, USA, 31 July–4 August 2006; pp. 2697–2700.
22. Dennison, P.E.; Brunelle, A.R.; Carter, V.A. Assessing canopy mortality during a mountain pine beetle outbreak using GeoEye-1 high spatial resolution satellite data. *Remote Sens. Environ.* **2010**, *114*, 2431–2435. [CrossRef]
23. Xue, J.; Su, B. Significant Remote Sensing Vegetation Indices: A Review of Developments and Applications. *J. Sens.* **2017**, *2017*, 1353691. [CrossRef]
24. Cheng, G.; Han, J. A survey on object detection in optical remote sensing images. *ISPRS J. Photogramm. Remote Sens.* **2016**, *117*, 11–28. [CrossRef]
25. Li, Z.; Liu, F.; Yang, W.; Peng, S.; Zhou, J. A Survey of Convolutional Neural Networks: Analysis, Applications, and Prospects. *IEEE Trans. Neural Netw. Learn. Syst.* **2022**, *33*, 6999–7019. [CrossRef] [PubMed]
26. Yu, R.; Luo, Y.; Zhou, Q.; Zhang, X.; Wu, D.; Ren, L. Early detection of pine wilt disease using deep learning algorithms and UAV-based multispectral imagery. *For. Ecol. Manag.* **2021**, *497*, 119493. [CrossRef]
27. Xia, L.; Zhang, R.; Chen, L.; Li, L.; Yi, T.; Wen, Y.; Ding, C.; Xie, C. Evaluation of Deep Learning Segmentation Models for Detection of Pine Wilt Disease in Unmanned Aerial Vehicle Images. *Remote Sens.* **2021**, *13*, 3594. [CrossRef]
28. Wu, B.; Liang, A.; Zhang, H.; Zhu, T.; Zou, Z.; Yang, D.; Tang, W.; Li, J.; Su, J. Application of conventional UAV-based high-throughput object detection to the early diagnosis of pine wilt disease by deep learning. *For. Ecol. Manag.* **2021**, *486*, 118986. [CrossRef]
29. Han, Z.; Hu, W.; Peng, S.; Lin, H.; Zhang, J.; Zhou, J.; Wang, P.; Dian, Y. Detection of Standing Dead Trees after Pine Wilt Disease Outbreak with Airborne Remote Sensing Imagery by Multi-Scale Spatial Attention Deep Learning and Gaussian Kernel Approach. *Remote Sens.* **2022**, *14*, 3075. [CrossRef]
30. Zhang, R.; Xia, L.; Chen, L. Recognition of wilt wood caused by pine wilt nematode based on U-Net network and unmanned aerial vehicle images. *Trans. Chin. Soc. Agric. Eng.* **2020**, *36*, 61–68.
31. Xu, X.; Tao, H.; Li, C. Detection and Location of Pine Wilt Disease Induced Dead Pine Trees Based on Faster R-CNN. *Trans. Chin. Soc. Agric. Mach.* **2020**, *51*, 228–236.
32. Tao, H.; Li, C.; Zhao, D.; Deng, S.; Hu, H.; Xu, X.; Jing, W. Deep learning-based dead pine tree detection from unmanned aerial vehicle images. *Int. J. Remote Sens.* **2020**, *41*, 8238–8255. [CrossRef]
33. Li, M.; Li, H.; Ding, X.; Wang, L.; Wang, X.; Chen, F. The Detection of Pine Wilt Disease: A Literature Review. *Int. J. Mol. Sci.* **2022**, *23*, 10797. [CrossRef]
34. Pun, T.B.; Thapa Magar, R.; Koech, R.; Owen, K.J.; Adorada, D.L. Emerging Trends and Technologies Used for the Identification, Detection, and Characterisation of Plant-Parasitic Nematode Infestation in Crops. *Plants* **2024**, *13*, 3041. [CrossRef] [PubMed]
35. Tahir, S.; Hassan, S.S.; Yang, L.; Ma, M.; Li, C. Detection Methods for Pine Wilt Disease: A Comprehensive Review. *Plants* **2024**, *13*, 2876. [CrossRef] [PubMed]
36. Yang, Z.Z.; Zhao, B.; Guo, J. Review on Behavior Studies of the Pine Wood Nematode. *J. Nanjing For. Univ. (Nat. Sci. Ed.)* **2003**, *27*, 87–92. [CrossRef]
37. Bo, G.; Kazuyoshi, F.; Jack, R.; Yuko, T. *Pine Wilt Disease*; Springer Japan: Tokyo, Japan, 2008; pp. 18–25.
38. Hu, S.-j.; Ning, T.; Fu, D.-y.; Haack, R.A.; Zhang, Z.; Chen, D.-d.; Ma, X.-y.; Ye, H. Dispersal of the Japanese Pine Sawyer, *Monochamus alternatus* (*Coleoptera*: *Cerambycidae*), in Mainland China as Inferred from Molecular Data and Associations to Indices of Human Activity. *PLoS ONE* **2013**, *8*, e57568. [CrossRef]
39. Hirata, A.; Nakamura, K.; Nakao, K.; Kominami, Y.; Tanaka, N.; Ohashi, H.; Takano, K.T.; Takeuchi, W.; Matsui, T. Potential distribution of pine wilt disease under future climate change scenarios. *PLoS ONE* **2017**, *12*, e0182837. [CrossRef]
40. Ye, J. Epidemic Status of Pine Wilt Disease in China and Its Prevention and Control Techniques and Counter Measures. *Sci. Silvae Sin.* **2019**, *55*, 267–276.
41. Clevers, J.; Kooistra, L. Using Hyperspectral Remote Sensing Data for Retrieving Canopy Chlorophyll and Nitrogen Content. *Ieee J. Sel. Top. Appl. Earth Obs. Remote Sens.* **2012**, *5*, 574–583. [CrossRef]
42. Koksal, E.S.; Ustun, H.; Ozcan, H.; Gunturk, A. Estimating Water Stressed Dwarf Green Bean Pigment Concentration Through Hyperspectral Indices. *Pak. J. Bot.* **2010**, *42*, 1895–1901.
43. dos Santos, C.S.S.; de Vasconcelos, M.W. Identification of genes differentially expressed in *Pinus pinaster* and *Pinus pinea* after infection with the pine wood nematode. *Eur. J. Plant Pathol.* **2012**, *132*, 407–418. [CrossRef]

44. Zhang, N.; Chai, X.; Li, N.; Zhang, J.; Sun, T. Applicability of UAV-based optical imagery and classification algorithms for detecting pine wilt disease at different infection stages. *GIScience Remote Sens.* **2023**, *60*, 2170479. [CrossRef]
45. Wu, D.; Yu, L.; Yu, R.; Zhou, Q.; Li, J.; Zhang, X.; Ren, L.; Luo, Y. Detection of the Monitoring Window for Pine Wilt Disease Using Multi-Temporal UAV-Based Multispectral Imagery and Machine Learning Algorithms. *Remote Sens.* **2023**, *15*, 444. [CrossRef]
46. van Halder, I.; Sacristan, A.; Martín-García, J.; Pajares, J.A.; Jactel, H. *Pinus pinea*: A natural barrier for the insect vector of the pine wood nematode? *Ann. For. Sci.* **2022**, *79*, 43. [CrossRef]
47. Robinet, C.; Castagnone-Sereno, P.; Mota, M.; Roux, G.; Sarniguet, C.; Tassus, X.; Jactel, H. Effectiveness of clear-cuttings in non-fragmented pine forests in relation to EU regulations for the eradication of the pine wood nematode. *J. Appl. Ecol.* **2020**, *57*, 460–466. [CrossRef]
48. Guo, Y.; Ma, J.; Sun, Y.; Carballar-Lejarazú, R.; Weng, M.; Shi, W.; Wu, J.; Hu, X.; Wang, R.; Zhang, F.; et al. Spatiotemporal dynamics of fluopyram trunk-injection in *Pinus massoniana* and its efficacy against pine wilt disease. *Pest Manag. Sci.* **2023**, *79*, 2230–2238. [CrossRef]
49. Xu, F. Recent Advances in the Integrated Management of the Pine Wood Nematode in China. In *Pine Wilt Disease*; Zhao, B.G., Futai, K., Sutherland, J.R., Takeuchi, Y., Eds.; Springer: Tokyo, Japan, 2008; pp. 323–333.
50. Guo, Y.; Lin, Q.; Chen, L.; Carballar-Lejarazú, R.; Zhang, A.; Shao, E.; Liang, G.; Hu, X.; Wang, R.; Xu, L.; et al. Characterization of bacterial communities associated with the pinewood nematode insect vector *Monochamus alternatus* Hope and the host tree *Pinus massoniana*. *BMC Genom.* **2020**, *21*, 337. [CrossRef]
51. Modesto, I.; Mendes, A.; Carrasquinho, I.; Miguel, C.M. Molecular Defense Response of Pine Trees (*Pinus* spp.) to the Parasitic Nematode *Bursaphelenchus xylophilus*. *Cells* **2022**, *11*, 3208. [CrossRef]
52. Prasad, A.K.; Chai, L.; Singh, R.P.; Kafatos, M. Crop yield estimation model for Iowa using remote sensing and surface parameters. *Int. J. Appl. Earth Obs. Geoinf.* **2006**, *8*, 26–33. [CrossRef]
53. Krishna, G.; Sahoo, R.N.; Singh, P.; Patra, H.; Bajpai, V.; Das, B.; Kumar, S.; Dhandapani, R.; Vishwakarma, C.; Pal, M.; et al. Application of thermal imaging and hyperspectral remote sensing for crop water deficit stress monitoring. *Geocarto Int.* **2021**, *36*, 481–498. [CrossRef]
54. Zhou, J.; Khot, L.R.; Boydston, R.A.; Miklas, P.N.; Porter, L. Low altitude remote sensing technologies for crop stress monitoring: A case study on spatial and temporal monitoring of irrigated pinto bean. *Precis. Agric.* **2018**, *19*, 555–569. [CrossRef]
55. Abd El-Ghany, N.M.; Abd El-Aziz, S.E.; Marei, S.S. A review: Application of remote sensing as a promising strategy for insect pests and diseases management. *Environ. Sci. Pollut. Res.* **2020**, *27*, 33503–33515. [CrossRef]
56. Yang, C. Remote Sensing and Precision Agriculture Technologies for Crop Disease Detection and Management with a Practical Application Example. *Engineering* **2020**, *6*, 528–532. [CrossRef]
57. Cavender-Bares, J.; Schneider, F.D.; Santos, M.J.; Armstrong, A.; Carnaval, A.; Dahlin, K.M.; Fatoyinbo, L.; Hurtt, G.C.; Schimel, D.; Townsend, P.A.; et al. Integrating remote sensing with ecology and evolution to advance biodiversity conservation. *Nat. Ecol. Evol.* **2022**, *6*, 506–519. [CrossRef] [PubMed]
58. Cotrozzi, L. Spectroscopic detection of forest diseases: A review (1970–2020). *J. For. Res.* **2022**, *33*, 21–38. [CrossRef]
59. Zhang, J.; Huang, Y.; Pu, R.; Gonzalez-Moreno, P.; Yuan, L.; Wu, K.; Huang, W. Monitoring plant diseases and pests through remote sensing technology: A review. *Comput. Electron. Agric.* **2019**, *165*, 104943. [CrossRef]
60. Kim, S.R.; Lee, W.K.; Lim, C.H.; Kim, M.; Kafatos, M.C.; Lee, S.H.; Lee, S.S. Hyperspectral Analysis of Pine Wilt Disease to Determine an Optimal Detection Index. *Forests* **2018**, *9*, 115. [CrossRef]
61. Wang, Z.; Zhang, X.; An, S. Spectral Characteristics Analysis of *Pinus massoniana* Suffered by *Bursaphelenchus Xylophilus*. *Remote Sens. Technol. Appl.* **2007**, *22*, 367–370.
62. Vogelmann, J.E.; Rock, B.N. Assessing forest damage in high-elevation coniferous forests in vermont and new Hampshire using thematic mapper data. *Remote Sens. Environ.* **1988**, *24*, 227–246. [CrossRef]
63. Xu, H.; Luo, Y. Changes of Reflectance Spectra of Pine Needles in Different Stage after Being Infected by Pine Wood Nematode. *Spectrosc. Spectr. Anal.* **2011**, *31*, 1352–1356.
64. Lee, J.B.; Kim, E.S.; Lee, S.H. An analysis of spectral pattern for detecting pine wilt disease using ground-based hyperspectral camera. *Korean J. Remote Sens.* **2014**, *30*, 665–675. [CrossRef]
65. Pan, J.; Lin, J.; Xie, T. Exploring the Potential of UAV-Based Hyperspectral Imagery on Pine Wilt Disease Detection: Influence of Spatio-Temporal Scales. *Remote Sens.* **2023**, *15*, 2281. [CrossRef]
66. Li, X.; Liu, Y.; Huang, P.; Tong, T.; Li, L.; Chen, Y.; Hou, T.; Su, Y.; Lv, X.; Fu, W.; et al. Integrating Multi-Scale Remote-Sensing Data to Monitor Severe Forest Infestation in Response to Pine Wilt Disease. *Remote Sens.* **2022**, *14*, 5164. [CrossRef]
67. Franklin, S.E.; Wulder, M.A.; Skakun, R.S.; Carroll, A.L. Mountain Pine Beetle Red-Attack Forest Damage Classification Using Stratified Landsat TM Data in British Columbia, Canada. *Photogramm. Eng. Remote Sens.* **2003**, *69*, 283–288. [CrossRef]
68. Long, L.; Chen, Y.; Song, S.; Zhang, X.; Jia, X.; Lu, Y.; Liu, G. Remote Sensing Monitoring of Pine Wilt Disease Based on Time-Series Remote Sensing Index. *Remote Sens.* **2023**, *15*, 360. [CrossRef]
69. White, J.C.; Wulder, M.A.; Grills, D. Detecting and mapping mountain pine beetle red-attack damage with SPOT-5 10-m multispectral imagery. *J. Ecosyst. Manag.* **2006**, *7*, 2. [CrossRef]
70. Hicke, J.A.; Logan, J. Mapping whitebark pine mortality caused by a mountain pine beetle outbreak with high spatial resolution satellite imagery. *Int. J. Remote Sens.* **2009**, *30*, 4427–4441. [CrossRef]

71. Poona, N.K.; Ismail, R. Discriminating the occurrence of pitch canker fungus in *Pinus* radiata trees using QuickBird imagery and artificial neural networks. *South. For. A J. For. Sci* **2013**, *75*, 1.
72. White, J.C.; Wulder, M.A.; Brooks, D.; Reich, R.; Wheate, R.D. Detection of red attack stage mountain pine beetle infestation with high spatial resolution satellite imagery. *Remote Sens. Environ.* **2005**, *96*, 340–351. [CrossRef]
73. Jo, M.H.; Kim, J.B.; Oh, J.S.; Lee, K.J. Extraction Method of Damaged Area by Pinetree Pest(*Bursaphelenchus Xylophilus*) using High Resolution IKONOS Image. *J. Korean Assoc. Geogr. Inf. Stud.* **2001**, *4*, 1–5.
74. Qiao, R.; Tang, P. Recognition of red-attack pine trees using WorldView-2 imagery. *J. Beijing For. Univ.* **2015**, *37*, 33–40. [CrossRef]
75. Kavzoglu, T.; Colkesen, I.; Yomralioglu, T. Object-based classification with rotation forest ensemble learning algorithm using very-high-resolution WorldView-2 image. *Remote Sens. Lett.* **2015**, *6*, 834–843. [CrossRef]
76. Cai, P.; Chen, G.; Yang, H.; Li, X.; Zhu, K.; Wang, T.; Liao, P.; Han, M.; Gong, Y.; Wang, Q.; et al. Detecting Individual Plants Infected with Pine Wilt Disease Using Drones and Satellite Imagery: A Case Study in Xianning, China. *Remote Sens.* **2023**, *15*, 2671. [CrossRef]
77. Zhou, H.; Yuan, X.; Zhou, H.; Shen, H.; Ma, L.; Sun, L.; Fang, G.; Sun, H. Surveillance of pine wilt disease by high resolution satellite. *J. For. Res.* **2022**, *33*, 1401–1408. [CrossRef]
78. Zhou, Z.; Li, R.; Ben, Z. Automatic identification of *Bursaphelenchus xylophilus* from remote sensing images using residual network. *J. For. Eng.* **2022**, *7*, 185–191. [CrossRef]
79. Huang, J.; Lu, X.; Chen, L.; Sun, H.; Wang, S.; Fang, G. Accurate Identification of Pine Wood Nematode Disease with a Deep Convolution Neural Network. *Remote Sens.* **2022**, *14*, 913. [CrossRef]
80. Meddens, A.J.H.; Hicke, J.A.; Vierling, L.A.; Hudak, A.T. Evaluating methods to detect bark beetle-caused tree mortality using single-date and multi-date Landsat imagery. *Remote Sens. Environ.* **2013**, *132*, 49–58. [CrossRef]
81. Sun, G.; Hu, T.; Chen, S.; Sun, J.; Zhang, J.; Ye, R.; Zhang, S.; Liu, J. Using UAV-based multispectral remote sensing imagery combined with DRIS method to diagnose leaf nitrogen nutrition status in a fertigated apple orchard. *Precis. Agric.* **2023**, *24*, 2522–2548. [CrossRef]
82. Zhang, J.; Xu, S.; Zhao, Y.; Sun, J.; Xu, S.; Zhang, X. Aerial orthoimage generation for UAV remote sensing: Review. *Inf. Fusion* **2023**, *89*, 91–120. [CrossRef]
83. Xia, L.; Zhang, R.; Chen, L.; Huang, Y.; Xu, G.; Wen, Y.; Yi, T. Monitor Cotton Budding Using SVM and UAV Images. *Appl. Sci.* **2019**, *9*, 4312. [CrossRef]
84. Hu, P.; Zhang, R.; Yang, J.; Chen, L. Development Status and Key Technologies of Plant Protection UAVs in China: A Review. *Drones* **2022**, *6*, 354. [CrossRef]
85. Zhang, B.; Ye, H.; Lu, W.; Huang, W.; Wu, B.; Hao, Z.; Sun, H. A Spatiotemporal Change Detection Method for Monitoring Pine Wilt Disease in a Complex Landscape Using High-Resolution Remote Sensing Imagery. *Remote Sens.* **2021**, *13*, 2083. [CrossRef]
86. Huang, H.; Ma, X.; Hu, L. The preliminary application of the combination of Fast R-CNN deep learning and UAV remote sensing in the monitoring of pine wilt disease. *J. Environ. Entomol.* **2021**, *43*, 1295–1303.
87. Zhang, L.; Zhang, L.; Du, B. Deep Learning for Remote Sensing Data: A Technical Tutorial on the State of the Art. *IEEE Geosci. Remote Sens. Mag.* **2016**, *4*, 22–40. [CrossRef]
88. Zhou, Y.; Liu, W.; Bi, H.; Chen, R.; Zong, S.; Luo, Y. A Detection Method for Individual Infected Pine Trees with Pine Wilt Disease Based on Deep Learning. *Forests* **2022**, *13*, 1880. [CrossRef]
89. Duarte, A.; Borralho, N.; Cabral, P.; Caetano, M. Recent Advances in Forest Insect Pests and Diseases Monitoring Using UAV-Based Data: A Systematic Review. *Forests* **2022**, *13*, 911. [CrossRef]
90. Wang, S.; Cao, X.; Wu, M.; Yi, C.; Zhang, Z.; Fei, H.; Zheng, H.; Jiang, H.; Jiang, Y.; Zhao, X.; et al. Detection of Pine Wilt Disease Using Drone Remote Sensing Imagery and Improved YOLOv8 Algorithm: A Case Study in Weihai, China. *Forests* **2023**, *14*, 2052. [CrossRef]
91. Park, H.G.; Yun, J.P.; Kim, M.Y.; Jeong, S.H. Multichannel Object Detection for Detecting Suspected Trees With Pine Wilt Disease Using Multispectral Drone Imagery. *IEEE J. Sel. Top. Appl. Earth Obs. Remote Sens.* **2021**, *14*, 8350–8358. [CrossRef]
92. Yu, R.; Luo, Y.; Li, H.; Yang, L.; Huang, H.; Yu, L.; Ren, L. Three-Dimensional Convolutional Neural Network Model for Early Detection of Pine Wilt Disease Using UAV-Based Hyperspectral Images. *Remote Sens.* **2021**, *13*, 4065. [CrossRef]
93. Yu, R.; Huo, L.; Huang, H.; Yuan, Y.; Gao, B.; Liu, Y.; Yu, L.; Li, H.; Yang, L.; Ren, L.; et al. Early detection of pine wilt disease tree candidates using time-series of spectral signatures. *Front. Plant Sci.* **2022**, *13*, 1000093. [CrossRef]
94. Li, J.; Wang, X.; Zhao, H.; Hu, X.; Zhong, Y. Detecting pine wilt disease at the pixel level from high spatial and spectral resolution UAV-borne imagery in complex forest landscapes using deep one-class classification. *Int. J. Appl. Earth Obs. Geoinf.* **2022**, *112*, 102947. [CrossRef]
95. Tao, H.; Li, C.; Xie, C. Recognition of red-attack pine trees from UAV imagery based on the HSV threshold method. *J. Nanjing For. Univ. (Nat. Sci. Ed.)* **2019**, *43*, 99–106.
96. Huang, L.; Wang, Y.; Xu, Q.; Liu, Q. Recognition of abnormally discolored trees caused by pine wilt disease using YOLO algorithm and UAV images. *Trans. Chin. Soc. Agric. Eng.* **2021**, *37*, 197–203.
97. You, J.; Zhang, R.; Lee, J. A Deep Learning-Based Generalized System for Detecting Pine Wilt Disease Using RGB-Based UAV Images. *Remote Sens.* **2022**, *14*, 150. [CrossRef]
98. Wu, K.; Zhang, J.; Yin, X.; Wen, S.; Lan, Y. An improved YOLO model for detecting trees suffering from pine wilt disease at different stages of infection. *Remote Sens. Lett.* **2023**, *14*, 114–123. [CrossRef]

99. Wan, J.; Wu, L.; Zhang, S.; Liu, S.; Xu, M.; Sheng, H.; Cui, J. Monitoring of Discolored Trees Caused by Pine Wilt Disease Based on Unsupervised Learning with Decision Fusion Using UAV Images. *Forests* **2022**, *13*, 1884. [CrossRef]
100. Chen, Y.; Yan, E.; Jiang, J.; Zhang, G.; Mo, D. An efficient approach to monitoring pine wilt disease severity based on random sampling plots and UAV imagery. *Ecol. Indic.* **2023**, *156*, 111215. [CrossRef]
101. Wang, G.; Zhao, H.; Chang, Q.; Lyu, S.; Liu, B.; Wang, C.; Feng, W. Detection Method of Infected Wood on Digital Orthophoto Map–Digital Surface Model Fusion Network. *Remote Sens.* **2023**, *15*, 4295. [CrossRef]
102. Qin, J.; Wang, B.; Wu, Y.; Lu, Q.; Zhu, H. Identifying Pine Wood Nematode Disease Using UAV Images and Deep Learning Algorithms. *Remote Sens.* **2021**, *13*, 162. [CrossRef]
103. Iordache, M.-D.; Mantas, V.; Baltazar, E.; Pauly, K.; Lewyckyj, N. A Machine Learning Approach to Detecting Pine Wilt Disease Using Airborne Spectral Imagery. *Remote Sens.* **2020**, *12*, 2280. [CrossRef]
104. Näsi, R.; Honkavaara, E.; Lyytikäinen-Saarenmaa, P.; Blomqvist, M.; Litkey, P.; Hakala, T.; Viljanen, N.; Kantola, T.; Tanhuanpää, T.; Holopainen, M. Using UAV-Based Photogrammetry and Hyperspectral Imaging for Mapping Bark Beetle Damage at Tree-Level. *Remote Sens.* **2015**, *7*, 15467–15493. [CrossRef]
105. Qin, B.; Sun, F.; Shen, W.; Dong, B.; Ma, S.; Huo, X.; Lan, P. Deep Learning-Based Pine Nematode Trees' Identification Using Multispectral and Visible UAV Imagery. *Drones* **2023**, *7*, 183. [CrossRef]
106. Yu, R.; Ren, L.; Luo, Y. Early detection of pine wilt disease in *Pinus* tabuliformis in North China using a field portable spectrometer and UAV-based hyperspectral imagery. *For. Ecosyst.* **2021**, *8*, 44. [CrossRef]
107. Li, H.; Chen, L.; Yao, Z.; Li, N.; Long, L.; Zhang, X. Intelligent Identification of Pine Wilt Disease Infected Individual Trees Using UAV-Based Hyperspectral Imagery. *Remote Sens.* **2023**, *15*, 3295. [CrossRef]
108. Zhang, S.; Huang, H.; Huang, Y.; Cheng, D.; Huang, J. A GA and SVM Classification Model for Pine Wilt Disease Detection Using UAV-Based Hyperspectral Imagery. *Appl. Sci.* **2022**, *12*, 6676. [CrossRef]
109. Liu, J.; Wang, C.; Cang, Y. Monitoring method of *Bursaphelenchus xylophilus* based on multi-eature CRF by UAV image. *Bull. Surv. Mapp.* **2019**, 78–82. [CrossRef]
110. Liu, C.; Sun, P.; Liu, S. A review of plant spectral reflectance response to water physiological changes. *Chin. J. Plant Ecol.* **2016**, *40*, 80–91.
111. Foley, W.J.; McIlwee, A.; Lawler, I.; Aragones, L.; Woolnough, A.P.; Berding, N. Ecological applications of near infrared reflectance spectroscopy—A tool for rapid, cost-effective prediction of the composition of plant and animal tissues and aspects of animal performance. *Oecologia* **1998**, *116*, 293–305. [CrossRef]
112. Verbesselt, J.; Hyndman, R.; Newnham, G.; Culvenor, D. Detecting trend and seasonal changes in satellite image time series. *Remote Sens. Environ.* **2010**, *114*, 106–115. [CrossRef]
113. Gitelson, A.A.; Merzlyak, M.N. Signature Analysis of Leaf Reflectance Spectra: Algorithm Development for Remote Sensing of Chlorophyll. *J. Plant Physiol.* **1996**, *148*, 494–500. [CrossRef]
114. Demetriades-Shah, T.H.; Steven, M.D.; Clark, J.A. High resolution derivative spectra in remote sensing. *Remote Sens. Environ.* **1990**, *33*, 55–64. [CrossRef]
115. Pearson, R.; Miller, L. Remote Mapping of Standing Crop Biomass for Estimation of Productivity of the Shortgrass Prairie. *Remote Sens. Environ.* **1972**, *355*, 1355.
116. Eitel, J.U.H.; Vierling, L.A.; Litvak, M.E.; Long, D.S.; Schulthess, U.; Ager, A.A.; Krofcheck, D.J.; Stoscheck, L. Broadband, red-edge information from satellites improves early stress detection in a New Mexico conifer woodland. *Remote Sens. Environ.* **2011**, *115*, 3640–3646. [CrossRef]
117. Gitelson, A.A.; Kaufman, Y.J.; Stark, R.; Rundquist, D. Novel algorithms for remote estimation of vegetation fraction. *Remote Sens. Environ.* **2002**, *80*, 76–87. [CrossRef]
118. Uto, K.; Takabayashi, Y.; Kosugi, Y.; Ogata, T. Hyperspectral Analysis of Japanese Oak Wilt to Determine Normalized Wilt Index. In Proceedings of the IGARSS 2008—2008 IEEE International Geoscience and Remote Sensing Symposium, Boston, MA, USA, 7–11 July 2008; pp. II-295–II-298.
119. Sims, D.A.; Gamon, J.A. Relationships between leaf pigment content and spectral reflectance across a wide range of species, leaf structures and developmental stages. *Remote Sens. Environ.* **2002**, *81*, 337–354. [CrossRef]
120. Houlès, V.; Guérif, M.; Mary, B. Elaboration of a nitrogen nutrition indicator for winter wheat based on leaf area index and chlorophyll content for making nitrogen recommendations. *Eur. J. Agron* **2007**, *27*, 1–11. [CrossRef]
121. Abdullah, H.; Skidmore, A.K.; Darvishzadeh, R.; Heurich, M. Timing of red-edge and shortwave infrared reflectance critical for early stress detection induced by bark beetle (*Ips typographus*, L.) attack. *Int. J. Appl. Earth Obs. Geoinf.* **2019**, *82*, 101900. [CrossRef]
122. Rouse, J.W.; Haas, R.H.; Schell, J.A.; Deering, D.W. Monitoring vegetation systems in the Great Plains with ERTS. *NASA Spec. Publ.* **1974**, *351*, 309.
123. Richardson, A.J.; Wiegand, C.L. Distinguishing vegetation from soil background information. *Photogramm. Eng. Remote Sens.* **1977**, *43*, 78A17199.
124. Gitelson, A.; Merzlyak, M.N. Spectral Reflectance Changes Associated with Autumn Senescence of Aesculus hippocastanum L. and Acer platanoides L. Leaves. Spectral Features and Relation to Chlorophyll Estimation. *J. Plant Physiol.* **1994**, *143*, 286–292. [CrossRef]
125. Assal, T.J.; Sibold, J.; Reich, R. Modeling a Historical Mountain Pine Beetle Outbreak Using Landsat MSS and Multiple Lines of Evidence. *Remote Sens. Environ.* **2014**, *155*, 275–288. [CrossRef]

126. Smith, R.; Adams, J.; Stephens, D.; Hick, P. Forecasting wheat yield in a Mediterranean-type environment from the NOAA satellite. *Aust. J. Agric. Res.* **1995**, *46*, 113–125. [CrossRef]
127. Merzlyak, M.N.; Gitelson, A.A.; Chivkunova, O.B.; Rakitin, V.Y. Non-destructive optical detection of pigment changes during leaf senescence and fruit ripening. *Physiol. Plant.* **1999**, *106*, 135–141. [CrossRef]
128. Hunt, E.R.; Rock, B.N. Detection of changes in leaf water content using Near- and Middle-Infrared reflectances. *Remote Sens. Environ.* **1989**, *30*, 43–54. [CrossRef]
129. Blackburn, G.A. Quantifying Chlorophylls and Caroteniods at Leaf and Canopy Scales: An Evaluation of Some Hyperspectral Approaches. *Remote Sens. Environ.* **1998**, *66*, 273–285. [CrossRef]
130. Carter, G.A.; Miller, R.L. Early detection of plant stress by digital imaging within narrow stress-sensitive wavebands. *Remote Sens. Environ.* **1994**, *50*, 295–302. [CrossRef]
131. Gao, B.-c. NDWI—A normalized difference water index for remote sensing of vegetation liquid water from space. *Remote Sens. Environ.* **1996**, *58*, 257–266. [CrossRef]
132. Fassnacht, F.E.; Latifi, H.; Ghosh, A.; Joshi, P.K.; Koch, B. Assessing the potential of hyperspectral imagery to map bark beetle-induced tree mortality. *Remote Sens. Environ.* **2014**, *140*, 533–548. [CrossRef]
133. Zhang, S.; Huang, J.; Hanan, J.; Qin, L. A hyperspectral GA-PLSR model for prediction of pine wilt disease. *Multimed. Tools Appl.* **2020**, *79*, 16645–16661. [CrossRef]
134. Li, H.; Liang, Y.; Xu, Q.; Cao, D. Key wavelengths screening using competitive adaptive reweighted sampling method for multivariate calibration. *Anal. Chim. Acta* **2009**, *648*, 77–84. [CrossRef]
135. Araújo, M.C.U.; Saldanha, T.C.B.; Galvão, R.K.H.; Yoneyama, T.; Chame, H.C.; Visani, V. The successive projections algorithm for variable selection in spectroscopic multicomponent analysis. *Chemom. Intell. Lab. Syst.* **2001**, *57*, 65–73. [CrossRef]
136. Li, N.; Huo, L.; Zhang, X. Classification of pine wilt disease at different infection stages by diagnostic hyperspectral bands. *Ecol. Indic.* **2022**, *142*, 109198. [CrossRef]
137. Zhang, N.; Zhang, X.; Yang, G.; Zhu, C.; Huo, L.; Feng, H. Assessment of defoliation during the Dendrolimus tabulaeformis Tsai et Liu disaster outbreak using UAV-based hyperspectral images. *Remote Sens. Environ.* **2018**, *217*, 323–339. [CrossRef]
138. Awad, M.M. Forest mapping: A comparison between hyperspectral and multispectral images and technologies. *J. For. Res.* **2018**, *29*, 1395–1405. [CrossRef]
139. Poona, N.K.; Ismail, R. Discriminating the occurrence of pitch canker infection in *Pinus* radiata forests using high spatial resolution QuickBird data and artificial neural networks. In Proceedings of the 2012 IEEE International Geoscience and remote sensing Symposium, Munich, Germany, 22–27 July 2012; pp. 3371–3374.
140. Kattenborn, T.; Leitloff, J.; Schiefer, F.; Hinz, S. Review on Convolutional Neural Networks (CNN) in vegetation remote sensing. *ISPRS J. Photogramm. Remote Sens.* **2021**, *173*, 24–49. [CrossRef]
141. Zahangir Alom, M.; Taha, T.M.; Yakopcic, C.; Westberg, S.; Sidike, P.; Shamima Nasrin, M.; Van Esesn, B.C.; Awwal, A.A.S.; Asari, V.K. The History Began from AlexNet: A Comprehensive Survey on Deep Learning Approaches. *arXiv* **2018**, arXiv:1803.01164. [CrossRef]
142. Al-Qizwini, M.; Barjasteh, I.; Al-Qassab, H.; Radha, H. Deep learning algorithm for autonomous driving using GoogLeNet. In Proceedings of the 2017 IEEE Intelligent Vehicles Symposium (IV), Los Angeles, CA, USA, 11–14 June 2017; pp. 89–96.
143. Ye, X.; Pan, J.; Shao, F.; Liu, G.; Lin, J.; Xu, D.; Liu, J. Exploring the potential of visual tracking and counting for trees infected with pine wilt disease based on improved YOLOv5 and StrongSORT algorithm. *Comput. Electron. Agric.* **2024**, *218*, 108671. [CrossRef]
144. Rao, D.; Zhang, D.; Lu, H.; Yang, Y.; Qiu, Y.; Ding, M.; Yu, X. Deep learning combined with Balance Mixup for the detection of pine wilt disease using multispectral imagery. *Comput. Electron. Agric.* **2023**, *208*, 107778. [CrossRef]
145. Padilla, R.; Netto, S.L.; Silva, E.A.B.d. A Survey on Performance Metrics for Object-Detection Algorithms. In Proceedings of the 2020 International Conference on Systems, Signals and Image Processing (IWSSIP), Niteroi, Brazil, 1–3 July 2020; pp. 237–242.
146. Tong, K.; Wu, Y. Rethinking PASCAL-VOC and MS-COCO dataset for small object detection. *J. Vis. Commun. Image Represent.* **2023**, *93*, 103830. [CrossRef]
147. Deng, X.; Tong, Z.; Lan, Y.; Huang, Z. Detection and Location of Dead Trees with Pine Wilt Disease Based on Deep Learning and UAV Remote Sensing. *Agriengineering* **2020**, *2*, 294–307. [CrossRef]
148. Sun, Z.; Ibrayim, M.; Hamdulla, A. Detection of Pine Wilt Nematode from Drone Images Using UAV. *Sensors* **2022**, *22*, 4704. [CrossRef]
149. Ren, D.; Peng, Y.; Sun, H.; Yu, M.; Yu, J.; Liu, Z. A Global Multi-Scale Channel Adaptation Network for Pine Wilt Disease Tree Detection on UAV Imagery by Circle Sampling. *Drones* **2022**, *6*, 353. [CrossRef]
150. Jung, Y.; Byun, S.; Kim, B.; Ul Amin, S.; Seo, S. Harnessing synthetic data for enhanced detection of Pine Wilt Disease: An image classification approach. *Comput. Electron. Agric.* **2024**, *218*, 108690. [CrossRef]
151. Li, H.; Fang, W.; Li, L.; Chen, X. Recognition of pine wood infected with pine nematode disease based on deep learning. *J. For. Eng.* **2021**, *6*, 142–147. [CrossRef]
152. Qiao, R.; Ghodsi, A.; Wu, H.; Chang, Y.; Wang, C. Simple weakly supervised deep learning pipeline for detecting individual red-attacked trees in VHR remote sensing images. *Remote Sens. Lett.* **2020**, *11*, 650–658. [CrossRef]
153. Wang, J.; Zhao, J.; Sun, H.; Lu, X.; Huang, J.; Wang, S.; Fang, G. Satellite Remote Sensing Identification of Discolored Standing Trees for Pine Wilt Disease Based on Semi-Supervised Deep Learning. *Remote Sens.* **2022**, *14*, 5936. [CrossRef]

154. Ye, W.; Lao, J.; Liu, Y.; Chang, C.-C.; Zhang, Z.; Li, H.; Zhou, H. Pine pest detection using remote sensing satellite images combined with a multi-scale attention-UNet model. *Ecol. Inform.* **2022**, *72*, 101906. [CrossRef]
155. Li, F.; Shen, W.; Wu, J. Study on the Detection Method for Pinewood Wilt DiseaseTreeBased on YOLOv3-CIoU. *J. Shandong Agric. Univ. (Nat. Sci. Ed.)* **2021**, *52*, 224–233.
156. Li, F.; Liu, Z.; Shen, W.; Wang, Y.; Wang, Y.; Ge, C.; Sun, F.; Lan, P. A Remote Sensing and Airborne Edge-Computing Based Detection System for Pine Wilt Disease. *IEEE Access* **2021**, *9*, 66346–66360. [CrossRef]
157. Yu, R.; Luo, Y.; Zhou, Q.; Zhang, X.; Wu, D.; Ren, L. A machine learning algorithm to detect pine wilt disease using UAV-based hyperspectral imagery and LiDAR data at the tree level. *Int. J. Appl. Earth Obs. Geoinf.* **2021**, *101*, 102363. [CrossRef]
158. Wang, Y.; Lin, L.; Zhao, Q.; Yue, T.; Meng, D.; Leung, Y. Compressive Sensing of Hyperspectral Images via Joint Tensor Tucker Decomposition and Weighted Total Variation Regularization. *IEEE Geosci. Remote Sens. Lett.* **2017**, *14*, 2457–2461. [CrossRef]
159. Zhao, R.; Wang, Q.; Shen, Y. Kronecker compressive sensing-based mechanism with fully independent sampling dimensions for hyperspectral imaging. *J. Electron. Imaging* **2015**, *24*, 063012. [CrossRef]